

Model-based control and estimation of cavity flow oscillations

Clarence W. Rowley

Vejapong Juttijudata

Abstract—Techniques for feedback control of oscillations in the flow past a cavity are presented. Low-order models are obtained using two methods (empirical Galerkin models, and a simple nonlinear oscillator model), and validated against 2D direct numerical simulations of the flow, which is actuated by a body force at the leading edge of the cavity. The models are used to construct dynamic observers, which reconstruct the flow state from a single pressure sensor, and perform much better than static estimators commonly used for flow estimation. Several control approaches are compared, including simple proportional control with a phase lag, LQG control using Galerkin models, and a dynamic phasor approach based on the work of Noack et al (2003). All three controllers are implemented in the full simulation, and able to reduce the amplitude of oscillations. The LQG regulator requires careful tuning, and the closed-loop behavior often does not match that predicted by the model, but the dynamic phasor approach eliminates the oscillations completely in the full simulation, with a transient response that matches that predicted by the low-order model.

I. INTRODUCTION

Cavity flows arise in several aerospace applications, such as landing gear wheel wells and weapons bays in military aircraft. The basic geometry is shown in Fig. 1, and often oscillations occur due to a natural feedback mechanism: a free shear layer spanning the cavity amplifies disturbances, which scatter into acoustic waves at the downstream corner, which in turn excite further disturbances in the shear layer. This process results in discrete resonant tones, at frequencies for which this acoustic feedback is in phase with the shear layer disturbances.

Using open-loop and closed-loop control to suppress the resulting oscillations has been of engineering interest for decades, but most control strategies have been either heuristic [1], adaptive [2], [3], or based on empirical models identified from frequency-response experiments [4], [5]. For an extensive review of open- and closed-loop control strategies for cavity flows, see [6], [7].

Our focus is on developing low-order models useful for control design. Since the equations governing the general, arbitrary motion of a fluid are nonlinear and high-dimensional (turbulent solutions exist), low-order models are necessarily valid only over a limited dynamic envelope, typically for a small region of phase space, and for a narrow range of frequencies. In this paper, we explore two different types of

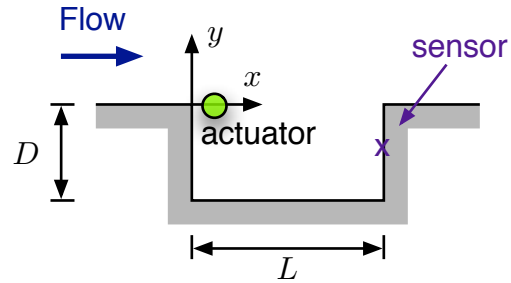


Fig. 1. Cavity flow geometry, showing location of sensor and actuator.

models, and control design techniques: empirical Galerkin models, with controllers designed using linear techniques such as LQR/LQG; and dynamic phasor models, after [8], [9], which are simple enough that custom-tailored control laws may be constructed that respect the range of validity of the models.

The models and feedback laws we obtain are tested on a Direct Numerical Simulation (DNS) of the two-dimensional flow geometry shown in Fig. 1. The flow conditions used here are for a Mach number of 0.6, $L/D = 2$, $Re_\theta = 56.8$ based on momentum thickness θ at the cavity leading edge, and $L/\theta = 52.8$. This simulation has been carefully validated using grid resolution and boundary placement studies, and comparison with experimental data [10]. The grid used 1008×384 gridpoints above the cavity and 240×96 gridpoints inside the cavity, which is sufficient to resolve all of the scales at this Reynolds number.

The organization of the paper is as follows: in §II we describe the empirical Galerkin model, and the dynamic observer and Linear Quadratic Regulator we obtain from it, and compare this controller to a simple proportional feedback, with a phase shift. In §III, we describe a model based on dynamic phasors, based on the approach in [8], [9], and the controller and observer based on this model.

II. EMPIRICAL GALERKIN MODELS

Galerkin models are obtained by projecting known dynamics (e.g., the Navier-Stokes equations) onto a smaller-dimensional subspace. Here, we start with the *isentropic* Navier-Stokes equations [11], written in two spatial dimen-

C.W. Rowley is with the Department of Mechanical and Aerospace Engineering, Princeton University, Princeton, NJ 08544, USA cwrowley@princeton.edu

V. Juttijudata is with the Department of Aerospace Engineering, Kasetsart University, Jatujak, Bangkok 10900, Thailand vejapong.j@gmail.com

sions as

$$\begin{aligned}\frac{\partial a}{\partial t} &= -v \cdot \nabla a - \frac{\gamma - 1}{2} a \nabla \cdot v \\ \frac{\partial v}{\partial t} &= -v \cdot \nabla v - \frac{2}{\gamma - 1} a \nabla a + \nu \nabla^2 v,\end{aligned}\quad (1)$$

where $v = (v_1, v_2)$ is the velocity, a is the local sound speed (which may be related to other flow variables, such as pressure, via isentropic relations), γ is the ratio of specific heats (1.4 for air), and ν is the kinematic viscosity, assumed constant (small density variations). These equations are quadratic in the flow variables, of the form

$$\dot{q} = L(q) + Q(q, q), \quad (2)$$

where $q = (v_1, v_2, a)$, L is a linear operator, and Q is bilinear (linear in each argument).

In order to include actuation in the model, we represent the actuator as a body force in the momentum equation. With actuation included, then, the model has the form

$$\dot{q} = L(q) + Q(q, q) + \sum_{j=1}^p \mathcal{B}_j u_j \quad (3)$$

where L and Q are the same as in (2), and where $\mathcal{B}_j(x, y)$ denotes the (spatially-dependent) body force introduced by the j -th actuator $u_j(t)$. Here, we will use a single actuator, with \mathcal{B}_1 oriented vertically (i.e., a body force in the y -direction), nonzero in a localized region in the shear layer (see Fig. 1), and zero elsewhere.

We expand the flow variables $q(x, y, t)$ in terms of basis functions $\varphi_j(x, y)$, as

$$q(x, y, t) = \bar{q}(x, y) + \sum_{j=1}^n z_j(t) \varphi_j(x, y), \quad (4)$$

where $\bar{q}(x)$ is some constant flow (typically a steady solution of Navier-Stokes, if known, or in our case a mean flow), and the z_j are time-varying coefficients. Thus, the *state* is the vector of coefficients $z = (z_1, \dots, z_n)$, and determining the state vector $z \in \mathbb{R}^n$ specifies the entire flow field q , according to (4). A *model* is then an evolution equation for $z(t)$.

Using the expansion (4), the model (3) has the form

$$\dot{z}_i(t) = c_i + A_{ij} z_j(t) + Q_{ijk} z_j(t) z_k(t) + B_{ij} u_j(t) \quad (5)$$

(summation implied), where

$$\begin{aligned}c_i &= \langle L(\bar{q}) + Q(\bar{q}, \bar{q}), \varphi_i \rangle \\ A_{ij} &= \langle L(\varphi_j) + Q(\bar{q}, \varphi_j) + Q(\varphi_j, \bar{q}), \varphi_i \rangle \\ Q_{ijk} &= \langle Q(\varphi_j, \varphi_k), \varphi_i \rangle \\ B_{ij} &= \langle \mathcal{B}_j, \varphi_i \rangle,\end{aligned}$$

where we have assumed the basis functions φ_j are orthonormal.

Generically, (5) may have many equilibrium points (e.g., even in one dimension, it may have zero, one, or two equilibria, or a continuum in degenerate cases), but for the cases we investigate, \bar{q} in (4) will already be “close” to an equilibrium point (albeit an unstable one), which will

imply that c_i is small, and there is a unique equilibrium point z^* close to the origin. In developing controllers, we will want to linearize about this equilibrium point, so writing $z(t) = z^* + \tilde{z}(t)$, one obtains

$$\dot{\tilde{z}}_i = \tilde{A}_{ij} \tilde{z}_j + Q_{ijk} \tilde{z}_j \tilde{z}_k + B_{ij} u_j, \quad (6)$$

where $\tilde{A}_{ij} = A_{ij} + (Q_{ijk} + Q_{ikj}) z_k^*$, so the linearized system is simply

$$\dot{\tilde{z}}_i = \tilde{A}_{ij} \tilde{z}_j + B_{ij} u_j. \quad (7)$$

A. Observer design

For implementation, it is not feasible to measure the state directly, so one must reconstruct the state from available sensor measurements, such as wall pressure. The sensor used in the observer is a pressure sensor in the downstream wall of the cavity, at $y = -0.5D$ (see Fig. 1). This sensor location was not optimized in any way, although one could consider optimal sensor placements by choosing sensor locations where the magnitudes of POD modes are large [12]. Each POD mode φ_j has a corresponding pressure p_j at this sensor location, and we represent the sensor signal $\eta(t)$ as

$$\eta(t) = \sum_{j=1}^n \tilde{z}_j(t) p_j = C \tilde{z}(t) \quad (8)$$

where C is the row vector $[p_1 \ \dots \ p_n]$.

For the model given by (6), one needs to specify basis functions φ_j , $j = 1, \dots, n$. For the observer design, we take $n = 4$ and determine the basis functions by Proper Orthogonal Decomposition (POD) of a dataset of snapshots from the natural (unforced) flow, and these four modes were sufficient to capture over 95% of the energy in the fluctuations [11].

We then design a Kalman filter [13] for the linearized system $\dot{\hat{z}} = \tilde{A} \hat{z}$, where \tilde{A} is the matrix from (6). Letting \hat{z} denote the estimate of the actual state \tilde{z} , the observer has the form

$$\dot{\hat{z}} = \tilde{A} \hat{z} + L(\eta - C \hat{z}) \quad (9)$$

where L is a matrix with n rows and one column (in general, if m sensors are available, L has m columns). For the Kalman filter design, the process noise variance is estimated from the size of the nonlinear terms in (6). There is very little noise in the pressure measurements in the simulation, but we expect much greater noise in experiments, so we artificially add random noise to the sensor signal, and use this noise variance for designing the Kalman filter gains. Once the observer weights are designed, we consider both the linear observer (9) and the nonlinear observer obtained by adding the correction $L(\eta - C \hat{z})$ to the nonlinear system (6).

In Fig. 2, we compare the performance of the Kalman filter with a commonly used method for state estimation in fluids, known as Linear Stochastic Estimation (LSE) [14], [15], which has recently been applied to cavity flows [16], [17], as well as cylinder wakes [12] and other flows [18]. In this method, one correlates sensor signals with full flow field information from a known database, and then uses the correlation to predict flow field information from the sensor

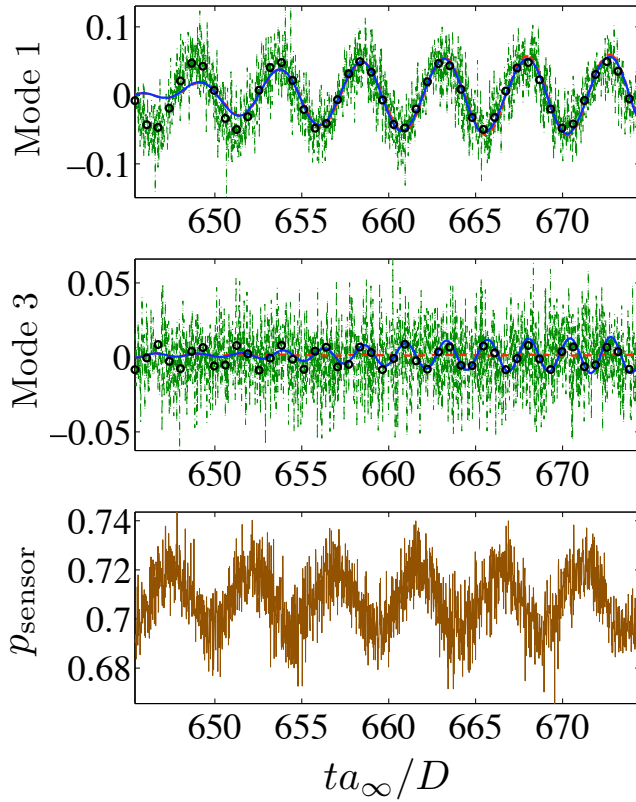


Fig. 2. Time traces of pressure sensor and POD modes 1 and 3, for exact projection of DNS (black \circ), linear observer using 1 sensor (red dashed); nonlinear observer using 1 sensor (blue solid); and LSE using three sensors (green dashed).

information, when the flow field is not directly available. Higher-order correlations are also possible, and Ukeiley has shown that quadratic stochastic estimation (QSE) outperforms LSE in predicting cavity flow fields [17].

The time traces shown in Fig. 2 show that both linear and nonlinear observers perform well, and accurately reconstruct the state from a single noisy pressure sensor. The nonlinear observer estimates the coefficients of mode 3 better, indicating that nonlinear coupling between modes 1–2 and modes 3–4 may be significant.

Figure 3 shows reconstructions of the full flow state at a particular time instant, comparing the full DNS solution with the estimate from the Kalman filter using a single (noisy) sensor, and LSE using three (noisy) sensors. The observer closely reproduces the flow structures in the full simulations. If clean sensors are used, the estimate from LSE is very close as well, but as seen in Fig. 3, when sensor noise is introduced, LSE can deviate substantially.

B. Controller design

Control design from Galerkin models is more challenging than observer design, because once actuation is introduced, typically the relevant flow structures change, so the basis functions φ_j need to include greater variety of spatial structures. To determine a model for control design, new POD modes were obtained from a richer variety of snap-

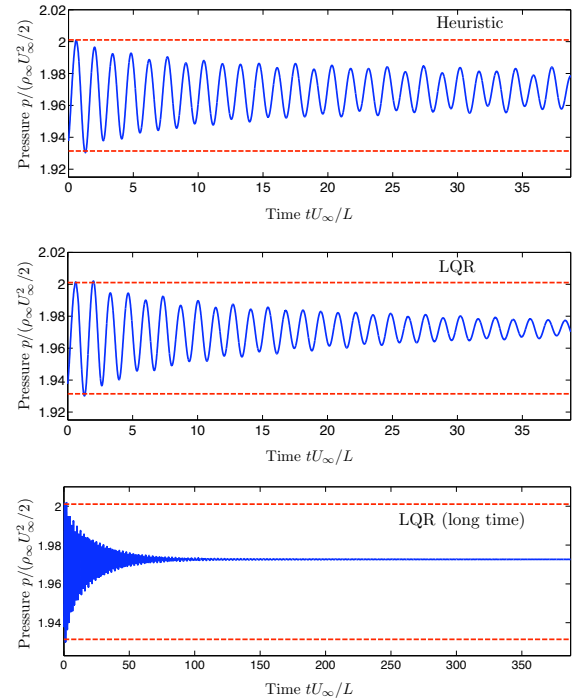


Fig. 4. Time traces from full DNS simulation: heuristic, proportional control (top), LQR (middle), and LQR for longer time scale (bottom). Red dashed lines indicate the extent of oscillations in the unforced flow.

shots, taken from simulations incorporating actuation using a heuristic, proportional feedback from the pressure sensor in the downstream wall at $y = -0.5D$ (this heuristic feedback law is described below). The first 10 POD modes were used, which together capture over 99.99% of the energy in the controlled flow.

The equations were then linearized about an equilibrium point of the model (5), and a state feedback $u = Kz$ was found using LQR. Several different weights in the LQR cost function were tried and implemented in the full DNS simulation, and most stabilized the model quite rapidly, but were less effective on the full simulation: usually the controller reduced the oscillation amplitude for a few cycles, but then the amplitude would grow larger than without forcing. Careful tuning could yield controllers which performed well on the full simulation, and the results of one of these are shown in Fig. 4, along with a heuristic, proportional controller, for comparison.

The heuristic control law was obtained by prescribing the body force to oppose the local velocity of the shear layer: if the shear layer has a positive vertical velocity, the body force is downward. The local velocity of the shear layer at the actuation point was correlated with the wall-pressure measurement, which was used as the sensor for the controller, and the corresponding phase delay was included in the feedback law.

As shown in Fig. 4, the LQR controller performs slightly better than the proportional controller. However, the results of the full simulation do not match those predicted by

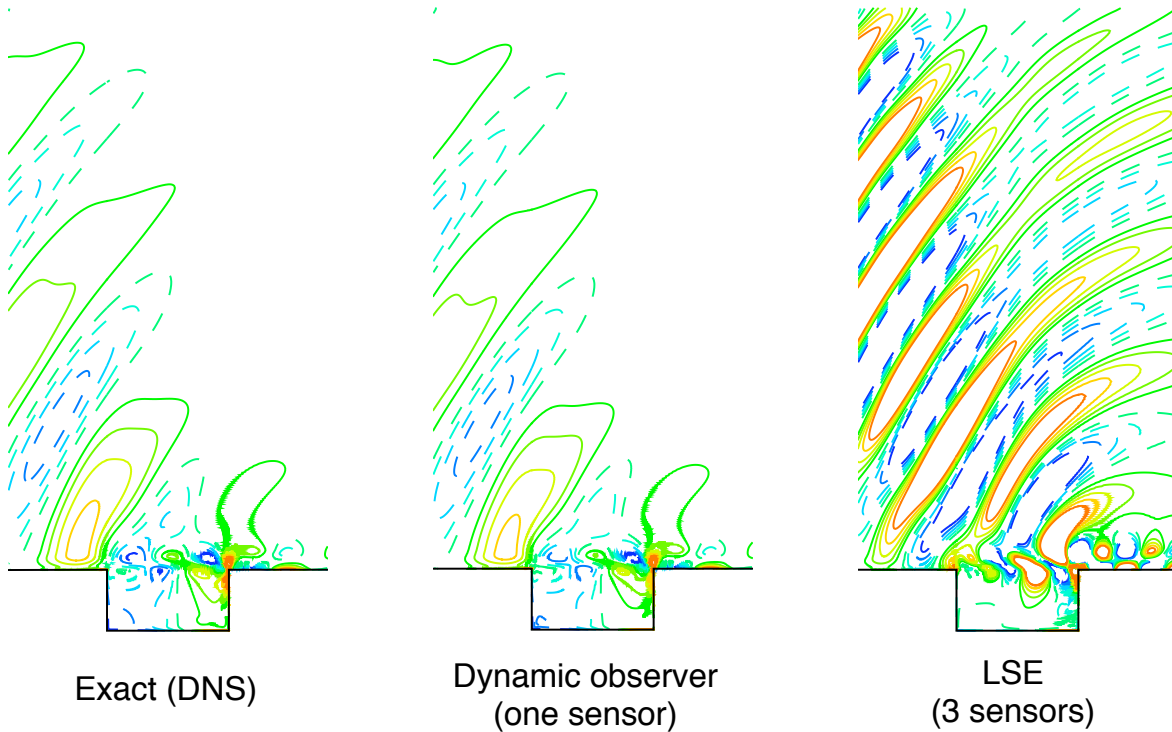


Fig. 3. Instantaneous contours of dilatation, from exact simulation (left), and estimates from dynamic observer (center) and Linear Stochastic Estimation (right), using noisy pressure signals.

the model (not shown), in which the feedback brings the amplitude close to zero with a settling time of about 2 cycles. The disagreement between model and full simulation is not surprising, however, because of the limited range of validity of the Galerkin models. Less aggressive LQR designs have little effect on the simulation, and more aggressive designs drive the system out of this range of validity. It is significant, however, that the feedback law shown in Fig. 4 stabilizes the full simulation for long time: these results indicate that stabilization is indeed possible for this flow, which is not necessarily the case for other flows, such as cylinder wakes [8].

III. DYNAMIC PHASOR MODELS

An alternative approach to modeling, inspired by the work of Tadmor, Noack, and others [8], [9], [19], [20], is to ignore the Navier-Stokes equations altogether, and postulate a low-order model that captures the relevant dynamical features of the flow. For instance, a simple dynamical system that describes oscillations at a frequency $\omega > 0$, is given by

$$\begin{aligned}\dot{r} &= \sigma r - \alpha r^3 \\ \dot{\theta} &= \omega\end{aligned}$$

where $\alpha > 0$ and σ are constants. In Cartesian coordinates, with $(a_1, a_2) = (r \cos \theta, r \sin \theta)$, and introducing a forcing term $u(t)$, the model takes the form

$$\dot{a} = A(r)a + Bu, \quad (10)$$

where $a = (a_1, a_2)$, $r = |a|$, and

$$A(r) = \begin{pmatrix} \sigma - \alpha r^2 & -\omega \\ \omega & \sigma - \alpha r^2 \end{pmatrix} \quad B = \begin{pmatrix} b_1 \\ b_2 \end{pmatrix}.$$

A model similar to this has been used for controlling cylinder wakes in [8], [9], [19], [20]. With no forcing ($u = 0$), with $\sigma \leq 0$, the origin is globally asymptotically stable, and with $\sigma > 0$, the origin is unstable, and there is a stable periodic orbit given by $r = \sqrt{\sigma/\alpha}$. This model is, of course, crude, and misses many of the details of the dynamics of cavity oscillations, but the goal is to obtain a model which is sufficient for control design, not to describe the cavity dynamics in a detailed way.

The parameters σ, α, ω are tuned to match simulations with no forcing, by observing the transient growth of oscillations from an initial condition near the unstable equilibrium point (of Navier-Stokes). The forcing parameters b_1, b_2 are then tuned to match simulations with small-amplitude sinusoidal forcing at a frequency close to the natural frequency ω .

A. Controller design

We wish to design a controller that stays within the range of validity of our model. Here, after [20], we consider a control input that is a sinusoid at the same frequency as the natural flow, with suitably chosen phase, and slowly-varying amplitude. In polar coordinates, (10) becomes

$$\begin{aligned}\dot{r} &= (\sigma - \alpha r^2)r + (b_1 \cos \theta + b_2 \sin \theta)u \\ \dot{\theta} &= \omega + \frac{1}{r}(b_2 \cos \theta - b_1 \sin \theta)u\end{aligned} \quad (11)$$

Now, let

$$u = r_c \cos(\theta - \theta_c),$$

where θ_c and r_c are controller parameters to be chosen. Assuming r is slowly varying, and inputs u are small, one may average over $\theta \in [0, 2\pi]$ (see [21]), and obtain the averaged equations

$$\begin{aligned} \dot{r} &= (\sigma - \alpha r^2)r + g_r \\ \dot{\theta} &= \omega + \frac{g_\theta}{r}, \end{aligned} \quad (12)$$

where

$$\begin{aligned} g_r &= \frac{r_c}{2}(b_1 \cos \theta_c + b_2 \sin \theta_c) \\ g_\theta &= \frac{r_c}{2}(b_2 \cos \theta_c - b_1 \sin \theta_c). \end{aligned}$$

If \dot{r} and $\dot{\theta} - \omega$ in (11) are $O(\varepsilon)$, then the averaging theorem states that solutions of (12) are ε -close to solutions of (11) for times $t \in [0, 1/\varepsilon]$. Choosing θ_c so that

$$\cos \theta_c = \frac{b_1}{|b|}, \quad \sin \theta_c = \frac{b_2}{|b|},$$

one obtains

$$g_r = r_c \frac{|b|}{2}, \quad g_\theta = 0.$$

One possible choice for r_c is then $r_c = -2\kappa r/|b|$, under which the closed-loop averaged equations (12) become

$$\begin{aligned} \dot{r} &= (\sigma - \kappa - \alpha r^2)r \\ \dot{\theta} &= \omega. \end{aligned} \quad (13)$$

By choosing $0 < \kappa < \sigma$, the amplitude of the periodic orbit decreases to $\sqrt{(\sigma - \kappa)/\alpha}$, and if $\kappa > \sigma$, then the origin becomes globally attracting, at least for the model. In the control design, however, we must not be too aggressive with the choice of κ , or we may leave the range of validity of the model.

B. Observer design

In order to implement the controller above, one needs estimates of r and θ . We use a very simple linear estimator, assuming $\dot{r} = 0$ in (12), to obtain an observer of the form

$$\begin{pmatrix} \dot{\hat{a}}_1 \\ \dot{\hat{a}}_2 \end{pmatrix} = \begin{pmatrix} 0 & -\omega \\ \omega & 0 \end{pmatrix} \begin{pmatrix} \hat{a}_1 \\ \hat{a}_2 \end{pmatrix} + \begin{pmatrix} b_1 \\ b_2 \end{pmatrix} u + \begin{pmatrix} L_1 \\ L_2 \end{pmatrix} (\eta - \hat{a}_1), \quad (14)$$

where η is the sensor measurement, which we have assumed measures a_1 directly (we may always change coordinates so that this is the case). Without inputs or sensor corrections, the model (14) has a one-parameter family of periodic orbits, all with period $2\pi/\omega$, so with sensor corrections, this model should track oscillations of any amplitude and phase, as long as the frequency is close to ω . For stability, we choose $L_1 > 0$, and choosing $L_2 = \omega - L_1^2/2\omega$ gives good transient behavior (critically damped poles of the error dynamics).

Full simulations reveal that, when control is introduced, the mean value of the sensed pressure drifts slowly, so a high-pass filter was used to remove this nonzero mean component.

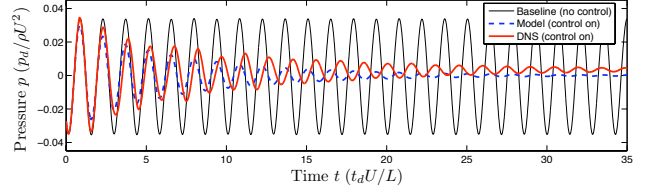


Fig. 5. Dynamic phasor controller: No forcing (black solid), model (blue dashed), and full DNS (red solid), with $\kappa = 2\sigma$.

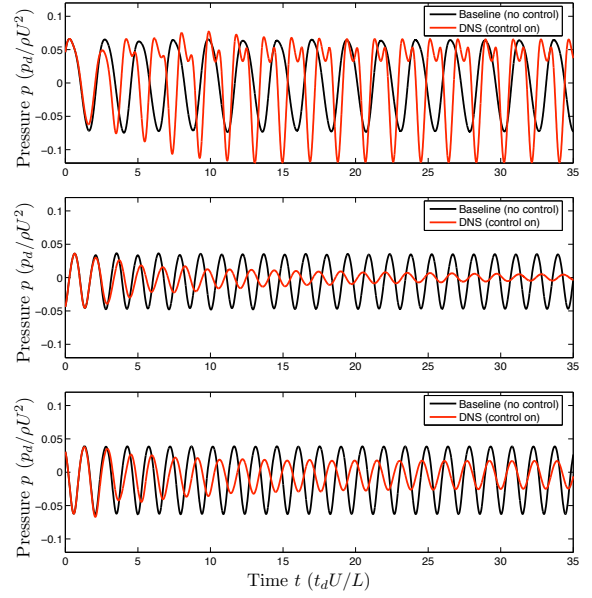


Fig. 7. Behavior of controller designed for $M = 0.6$ at off-design Mach numbers of $M = 0.55$ (top), $M = 0.65$ (middle); and $M = 0.70$ (bottom).

C. Results

Figure 5 shows the results of a controller and observer with $\kappa = 2\sigma$, and $L_1 = 1$. The behavior predicted by the model (13) is shown, and compared to the results of the full DNS simulation. The full simulation matches the model well, and remarkably, the amplitude of oscillations continues to decrease until a steady state is reached. The full simulations have been run until time $t = 120$, in the units in Fig. 5, and oscillations are virtually eliminated by time $t = 60$. The steady state reached is shown in Fig. 6, and looks similar to the time average of the uncontrolled flow. Different gains were also tried in the full simulation. For $\kappa/\sigma = 0.5$, the amplitude of oscillations was reduced, but not eliminated, while for $\kappa/\sigma \in [1, 3]$ the oscillations were eliminated completely. For $\kappa = 5\sigma$ the controller was too aggressive, and increased the amplitude of oscillations, deviating from the behavior predicted by the model.

As the Mach number varies, the frequency of oscillation changes, so one would not expect this controller to be very robust to changes in Mach number. Figure 7 shows the behavior of the controller designed for $M = 0.6$, when used at off-design flow conditions. As shown, for $M = 0.55$, the controller increases the amplitude of oscillations, while for

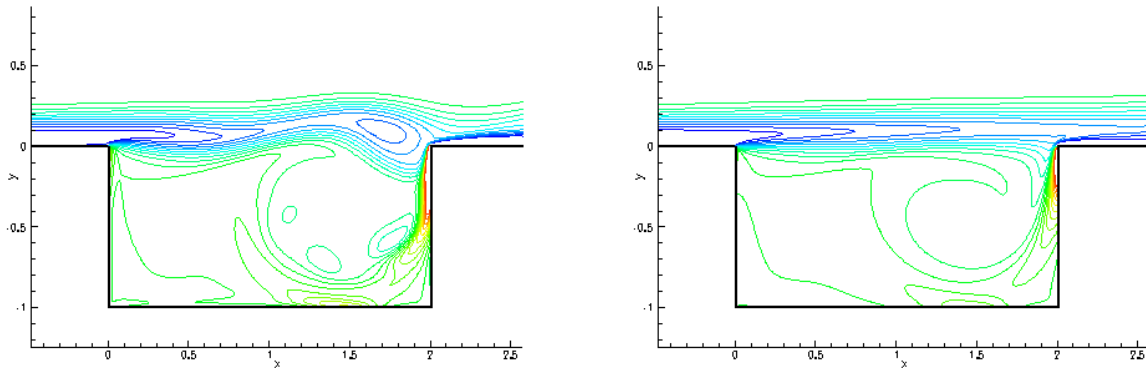


Fig. 6. Instantaneous vorticity contours before controller is turned on (left), and with phasor-based controller (right). The flow at right is steady, indicating that this is an equilibrium of Navier-Stokes, stabilized by the controller.

$M = 0.65$ and 0.70 , the controller reduces the amplitude slightly, but does not stabilize.

IV. CONCLUSIONS

Observers and feedback laws for suppressing oscillations in the flow past a cavity were presented using two different modeling techniques: empirical Galerkin models, and a dynamic phasor model. The Galerkin models work well for state estimation, but can be unreliable for control design, because of their very limited envelope of validity. Controllers designed from the dynamic phasor model were able to suppress oscillations completely, matching the behavior predicted by the model, as long as the control design was not too aggressive. This steady state was reached and maintained with zero average force being supplied by the actuator, only with small oscillatory forces that decrease with the amplitude of oscillations.

Of course, in experiments in which turbulence is present, one would not expect such a simple controller to be able to stabilize the flow, as this would imply removing all turbulence. However, it is reasonable to expect that a similar control design could suppress the primary resonance mechanism for cavity oscillations, and therefore significantly reduce the tones produced.

ACKNOWLEDGMENTS

This work was partially supported by AFOSR, under program managers Sharon Heise and John Schmisser. The authors gratefully acknowledge helpful advice from Gilead Tadmor, who suggested the use of the dynamic phasor model, and many interactions with Dave Williams, Tim Colonius, and Bernd Noack.

REFERENCES

- [1] M. Gharib, "Response of the cavity shear layer oscillations to external forcing," *AIAA J.*, vol. 25, no. 1, pp. 43–47, Jan. 1987.
- [2] L. N. Cattafesta, III, D. Shukla, S. Garg, and J. A. Ross, "Development of an adaptive weapons-bay suppression system," AIAA Paper 99-1901, May 1999.
- [3] M. A. Kegerise, R. H. Cabell, and L. N. Cattafesta, "Real-time adaptive control of flow-induced cavity tones," AIAA Paper 2004-0572, 2004.
- [4] L. N. Cattafesta, III, S. Garg, M. Choudhari, and F. Li, "Active control of flow-induced cavity resonance," AIAA Paper 97-1804, June 1997.
- [5] R. H. Cabell, M. A. Kegerise, D. E. Cox, and G. P. Gibbs, "Experimental feedback control of flow induced cavity tones," AIAA Paper 2002-2497, June 2002.
- [6] L. Cattafesta, D. R. Williams, C. W. Rowley, and F. Alvi, "Review of active control of flow-induced cavity resonance," AIAA Paper 2003-3567, June 2003.
- [7] C. W. Rowley and D. R. Williams, "Dynamics and control of high-reynolds-number flow over open cavities," *Annual Reviews of Fluid Mechanics*, January 2006.
- [8] B. Noack, K. Afanasiev, M. Morzyński, G. Tadmor, and F. Thiele, "A hierarchy of low-dimensional models for the transient and post-transient cylinder wake," *J. Fluid Mech.*, vol. 497, pp. 335–363, 2003.
- [9] G. Tadmor, B. Noack, A. Dillmann, J. Gerhard, M. Pastoor, R. King, and M. Morzyński, "Control, observation and energy regulation of wake flow instabilities," in *42nd IEEE Conference on Decision and Control*, Maui, HI, U.S.A., 9–12, Dec. 2003, pp. 2334–2339, weM10-4.
- [10] C. W. Rowley, T. Colonius, and A. J. Basu, "On self-sustained oscillations in two-dimensional compressible flow over rectangular cavities," *J. Fluid Mech.*, vol. 455, pp. 315–346, 2002.
- [11] C. W. Rowley, T. Colonius, and R. M. Murray, "Model reduction for compressible flow using POD and Galerkin projection," *Phys. D*, vol. 189, no. 1–2, pp. 115–129, Feb. 2004.
- [12] K. Cohen, S. Siegel, M. Luchtenburg, and T. McLaughlin, "Sensor placement for closed-loop flow control of a d-shaped cylinder wake," AIAA Paper 2004-2523, June 2004.
- [13] K. Zhou, J. C. Doyle, and K. Glover, *Robust and Optimal Control*. New Jersey: Prentice-Hall, 1996.
- [14] R. J. Adrian, B. G. Jones, M. K. Chung, Y. Hassan, C. K. Nothianandan, and A. T.-C. Tung, "Approximation of turbulent conditional averages by stochastic estimation," *Phys. Fluids A*, vol. 1, no. 6, 1989.
- [15] Y. Guezennec, "Stochastic estimation of coherent structures in turbulent boundary layers," *Phys. Fluids A*, vol. 1, no. 6, pp. 1054–1060, 1997.
- [16] N. E. Murray and L. S. Ukeiley, "Estimation of the flowfield from surface pressure measurements in an open cavity," *AIAA J.*, vol. 41, no. 5, pp. 969–972, 2003.
- [17] —, "Low-dimensional estimation of cavity flow dynamics," AIAA Paper 2004-681, 2004.
- [18] M. N. Glauser, H. Higuchi, J. Ausseur, and J. Pinier, "Feedback control of separated flows," AIAA Paper 2004-2521, June 2004.
- [19] B. Noack, G. Tadmor, and M. Morzyński, "Low-dimensional models for feedback flow control. part i: Empirical Galerkin models," in *2nd AIAA Flow Control Conference*, Portland, Oregon, U.S.A., June 28 – July 1, 2004, aIAA Paper 2004-2408 (invited contribution).
- [20] G. Tadmor, B. Noack, M. Morzyński, and S. Siegel, "Low-dimensional models for feedback flow control. Part II: Controller design and dynamic estimation," in *2nd AIAA Flow Control Conference*, Portland, Oregon, U.S.A., June 28 – July 1, 2004, aIAA Paper 2004-2409 (invited contribution).
- [21] J. Guckenheimer and P. J. Holmes, *Nonlinear Oscillations, Dynamical Systems, and Bifurcations of Vector Fields*, ser. Applied Mathematical Sciences. New York: Springer-Verlag, 1983, vol. 42.